The Influence of Lubricant Compressibility on the Performance of the 120 Degree Partial Journal Bearing

E. J. GUNTER, JR.
Associate Professor,
Department of Mechanical Engineering,
University of Virginia, Charlottesville, Va.;
Consultant to Friction and Lubrication Division,
The Franklin Institute,
Philadelphia, Pa. Mem. ASME

This paper discusses the characteristics of the 120 deg bearing as the compressibility parameter Λ is increased from 0 to ∞. At low values of Λ and light loads, the gas bearing behaves as an incompressible lubricated bearing. Curves are developed to show under what conditions of bearing loading, film thickness, and speed the partial gas bearing may be treated by the incompressible theory. The compressibility parameter Λ has a considerable effect on the proper selection of the shoe pivot position and bearing clearance ratio for both maximum load capacity and minimum coefficient of friction. It is shown that the bearing clearance ratio and pivot location can vary considerably and still maintain close to optimum conditions at low compressibility numbers. At higher compressibility numbers, the choice of pivot location has a substantial effect on the bearing load capacity and coefficient of friction. Also discussed are the optimum design ranges of the compressibility number Λ.

Introduction

In the last several years, the applications of gas bearings for high-speed turborotors have increased tremendously. For example, two important areas which have employed these bearings are helium compressors for nuclear reactors and turborotors for space power systems. One bearing configuration in particular has proved itself ideally suited for such applications because of its high stability and relative freedom from self-excited whirling. This bearing type is the self-acting tilting-pad partial journal bearing. This bearing arrangement has the additional advantage of being self-aligning. Also, by spring mounting one shoe, it can compensate for thermal effects and, in addition, has the capability of operation under a zero gravitational environment.

Since the governing Reynolds' equation for the partial gas bearing is nonlinear, the problem of analysis and design represents a formidable task. In the case of incompressible lubrication, the bearing characteristics may be represented by a single performance map based on the Sommerfeld number. The gas bearing requires field maps for each value of the compressibility parameter Λ. As each map requires several hours of high-speed digital computer time to develop, the analysis of the bearing behavior over a wide speed range represents an extremely time-consuming and costly procedure.

It is the purpose of this paper to present performance curves of the 120 deg bearing to represent the complete range of compressibility numbers from 0 to ∞; to show the optimum bearing conditions; and to demonstrate under what conditions the partial gas bearing may be approximated by linear incompressible theory.

Contributed by the Lubrication Division and presented at the Winter Annual Meeting, New York, N. Y., November 27–December 1, 1966, of The American Society of Mechanical Engineers. Manuscript received at ASME Headquarters, August 1, 1966. Paper No. 66—WA/Lub-2.

Analysis

The Reynolds' Equation

The general equation governing the steady-state pressure distribution between a rotating journal and bearing is given by Reynolds' equation [1][1]:

[1] Numbers in brackets designate References at end of paper.

Nomenclature

B = bearing length = $R\alpha$, in.
C = radial clearance between shoe and shaft = $R_{shoe} - R_{shaft}$, in.
C_f = friction factor, dimensionless
C_L = load coefficient = $W/Pa\ RL$, dimensionless
C_{Lc} = tangential load coefficient = $W_c/P_a\ RL$, dimensionless
C_{Ls} = normal load coefficient = W_s/P_aRL
C_0 = reference clearance, in.
F_f = shoe frictional force, lb
H = dimensionless film thickness = h/C
H_m = dimensionless minimum film thickness = $1 + \epsilon \cos(\xi + \alpha)$; $\xi + \alpha < 180$ deg or $= 1 - \epsilon$; $\xi + \alpha > 180$ deg
H_t = dimensionless trailing-edge film thickness = $1 + \epsilon \cos(\xi + \alpha) \times h_t/C$
L = shoe width, in.
N = shaft rotational speed, rpm
P = dimensionless pressure = p/P_a
P_a = ambient pressure, psi'
$\bar{P}$ = dimensionless perturbated pressure
Pj = journal unit loading = W/DL, dimensionless
R = shaft radius, in.
S = Sommerfeld number = $\dfrac{\mu N}{P_j}\left(\dfrac{R}{C}\right)^2$
v = specific volume
W = total bearing load, lb
Wc = tangential load, lb
Ws = normal load, lb
h_m = minimum film thickness, in.
h_t = trailing-edge film thickness, in.
Z = viscosity, centipoises
α = shoe arc length, deg
β = gas coefficient
ϵ = eccentricity ratio of shoe and shaft
η = dimensionless axial coordinate
θ = angle from line of centers to any shoe position in question, deg
Λ = bearing compressibility number = $6\ \mu\omega R^2/PaC^2$
μ = absolute lubricant viscosity, lb sec/sq in.
ρ = fluid density
ξ = angle between line of centers and shoe leading edge, deg
ϕ = angle between shoe leading edge and pivot, deg
ω = angular velocity, rad/sec
ψ = center of pressure measured from shoe leading edge
ϵ = shear stress

$$\frac{\partial}{\partial\theta}\left[\rho H^3\frac{\partial P}{\partial\theta}\right]+\left(\frac{R}{L}\right)^2\frac{\partial}{\partial\eta}\left[\rho H^3\frac{\partial P}{\partial n}\right]=\Lambda\frac{\partial}{\partial\theta}[\rho H] \quad (1)$$

Introducing the equation of state,

$$Pv^k = C \quad (2)$$

or in terms of density,

$$\rho = P^\beta$$

equation (1) becomes

$$\frac{\partial}{\partial\theta}\left[P^\beta H^3\frac{\partial P}{\partial\theta}\right]+\left(\frac{R}{L}\right)^2\frac{\partial}{\partial\eta}\left[P^\beta H^3\frac{\partial P}{\partial\eta}\right]=\Lambda\frac{\partial}{\partial\theta}[P^\beta H] \quad (3)$$

Let

$$P = p/p_a = 1 + \bar{P} \quad (4)$$

Expanding P^β in a binomial expansion and neglecting higher-order terms results in

$$\frac{\partial}{\partial\theta}\left[(1+\beta\bar{P})H^3\frac{\partial\bar{P}}{\partial\theta}\right]+\left(\frac{R}{L}\right)^2\frac{\partial}{\partial\eta}\left[(1+\cdot\beta\bar{P})H^3\frac{\partial\bar{P}}{\partial\eta}\right]$$
$$=\Lambda\frac{\partial}{\partial\theta}[(1+\beta\bar{P})H] \quad (5)$$

For the case of an incompressible fluid, β is identically equal to zero and equation (4) reduces to the standard linear Reynolds' equation for incompressible lubrication.

For the normal gas-lubricated bearing application, the equation of state is assumed to be isothermal and β is equal to 1. Equation (4) represents the perturbated Reynolds' equation for small changes of the bearing pressure above ambient. Thus it is obvious upon examination of equation (4) that, if the maximum bearing pressure rise as well as the average bearing unit loading are small in comparison to ambient pressure ($P_{\max} \ll 1$, $C_L \ll 1$), the bearing may be closely approximated by incompressible theory.

In order to calculate the gas bearing load capacity and film-thickness characteristics at various speeds, it is necessary to have numerous computer field maps such as those shown in Figs. 3–10. Since each field map (depending upon the compressibility parameter Λ) requires 1–2 hr of high-speed digital computer time to obtain, the complete analysis of a gas bearing becomes a costly and time-consuming procedure.

In certain applications in which the ambient pressure is high and the bearing loads are low, a wide range of the performance may be adequately estimated from incompressible theory. The conditions under which this approximation is valid will be developed in the following sections.

Equation (1) was reduced to a finite-difference equation and solved by digital computer. Reference [2] discusses in detail the method of solution of the finite-difference equations and the convergence criterion used. Also presented is a series of load and film-thickness performance curves for the 94.5 deg partial bearing for Λ ranging from 1.5 to 4.0.

Partial Journal Load Capacity

The bearing load capacity is obtained by integrating the shoe pressure profile along the bearing arc. Because of the shoe curvature, the load vector is divided into two components: A component perpendicular to the shoe-shaft line of centers W_s and a component parallel to the shoe-shaft line of centers W_c (see Fig. 1).

The dimensionless load coefficients are given by

$$C_{Lc} = \frac{Wc}{PaRL} = \int_{-1/2}^{1/2}\int_{\xi}^{\xi+\alpha}(P-1)\cos\theta\, d\theta\, d\eta \quad (6)$$

$$C_{Ls} = \frac{Ws}{PaRL} = \int_{-1/2}^{1/2}\int_{\xi}^{\xi+\alpha}(P-1)\sin\theta\, d\theta\, d\eta \quad (7)$$

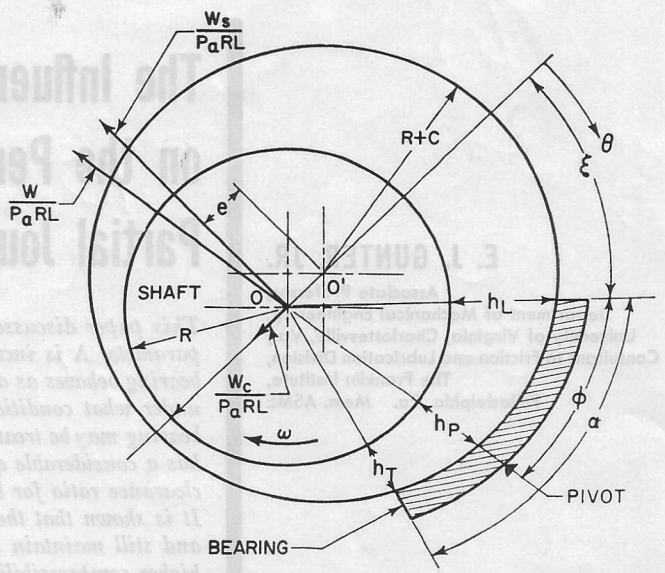

Fig. 1 Individual shoe-shaft bearing geometry

and the total bearing load coefficient is given by

$$C_L = \frac{W}{PaRL} = [C_{Lc}^2 + C_{Ls}^2]^{1/2} \quad (8)$$

The resultant center of pressure at which the total hydrodynamic bearing force acts can be determined from the radial and tangential load coefficients by the following equation:

$$\psi = 90 \text{ deg} - (\xi + \delta) \quad (9)$$

where

ψ = center of pressure measured from shoe leading edge
ξ = specified shoe lead angle (see Fig. 1)
$\delta = \tan^{-1}(C_{Lc}/C_{Ls})$

In a tilting-pad journal bearing, the sum of the moments about the pivot point due to the pressure forces and shearing tractions acting on the pad must be zero under equilibrium or steady-state conditions. In practice, the pad pivot position is not located at the journal surface but is at some distance d from the surface. Thus the influence of the bearing surface shearing stresses causes the center of pressure to be located slightly offset from the pivot position Φ.

The equilibrium condition between the pressure and shearing traction moments is given by

$$\frac{\Lambda}{6}\left(\frac{C}{R}\right)\int_{-1/2}^{1/2}\int_{\xi}^{\xi+\alpha}\left[1-\left(1+\frac{d}{R}\right)\cos(\Phi+\xi-\theta)\right]$$
$$\times\left(\frac{1}{H}+\frac{3H}{\Lambda}\frac{\partial P}{\partial\theta}\right)d\theta d\eta = \left(1+\frac{d}{R}\right)$$
$$\times[C_{Ls}\cos(\xi+\Phi) - C_{Lc}\sin(\xi+\Phi)] \quad (10)$$

where

d = radial location of pivot from journal bearing surface
$H = h/c = 1 + \epsilon\cos\theta$ = dimensionless film thickness
Φ = circumferential pivot location measured from shoe leading edge

In general, equation (10) requires an iterative method of solution in order to determine the shoe or pad center of pressure for a given pivot position and pivot film thickness. Investigation of the left-hand side of equation (10), which represents the shearing stress moments, indicates that this is usually of order C/R in

comparison to the pressure moments and thus may be neglected.

Equation (10) reduces to

$$C_{Ls} \cos (\xi + \Phi) - C_{Lc} \sin (\xi + \Phi) = 0 \qquad (11)$$

Solving for Φ,

$$\tan (\xi + \Phi) = C_{Ls}/C_{Lc} = \tan (90 \text{ deg} - \delta)$$

$$\therefore \Phi = 90 \text{ deg} - (\xi + \delta) = \psi \qquad (12)$$

Thus, in normal pivoted partial journal bearing applications, where the influence of the shearing stress terms on shoe equilibrium may be neglected and provided $d/R < 1$, the resultant center of pressure will correspond to location of the physical pivot.

Discussion

The variables used to develop the characteristic curves as depicted by Figs. 3–10 are the eccentricity ratio ϵ and the shoe lead angle ξ. For a given value of the compressibility parameter Λ, a complete characteristic curve is obtained by selecting numerous combinations of ϵ and ξ. For each set of values of ϵ and ξ, there are obtained a corresponding dimensionless load and the position or center of pressure at which the resultant load acts.

Because of the influence of compressibility, the bearing load is not directly proportional to speed or Λ. This requires a series of charts to completely describe the shoe performance over a range of speeds for a given shoe aspect ratio R/L. This differs from an incompressible fluid where a single field plot based on the Sommerfeld number completely describes the bearing characteristics over a range of speeds and loads. Performance curves for the 120 deg partial journal bearing have been developed for values of the compressibility parameter varying from 0 to ∞.

The incompressible bearing data of Raimondi is used to approximate the gas bearing behavior for low Λ and load conditions. The incompressible bearing data assume cavitation in the converging-diverging film section, which is an additional complication that is not present in the gas bearing. In normal gas pivoted-pad bearing applications, in which the pivot location exceeds 0.6, the low Λ film is converging and thus Fig. 3 may be used to adequately predict the bearing performance in this region.

Regions of Compressibility

The steady-state characteristics of a partial arc gas bearing may be classified into three regions of compressibility. The ranges of compressibility are approximately defined according to the compressibility numbers Λ and Λ_m, where Λ_m is defined as Λ/H_m.[2]

The regions of compressibility are as follows:

1 Approaching incompressible behavior.
2 Intermediate compressibility region.
3 Approaching compressibility limit.

In the first region, the effect of compressibility is negligible; in the second region, its influence is moderate; and in the third region, it predominates. These various ranges of compressibility are best illustrated by Fig. 2, which represents the shoe center-line pressure profiles for various values of Λ. (A similar figure for the 94.5 deg partial bearing is shown in reference [2].)

The convergence criterion of the present computer program and the accuracy of the data are greatly dependent upon the region of compressibility. For example, it is difficult to obtain accurate computer data at both high and low compressibility numbers, such as when $\Lambda < 1$ or $\Lambda > 20$.

The first compressibility range represents the limiting case where the gas bearing is approaching the incompressible behavior. This usually occurs in bearing applications which have such operating conditions as high ambient pressure, low loading, low speed, or large clearance ratios. Note that a gas bearing can be operating below $\Lambda = 1$ and still show considerable compressibility effects. Gross [1] shows that, for incompressibility, the compressibility number Λ_m based on minimum film thickness must be less than 10 for the flat slider bearing. This is also valid for the partial journal bearing.

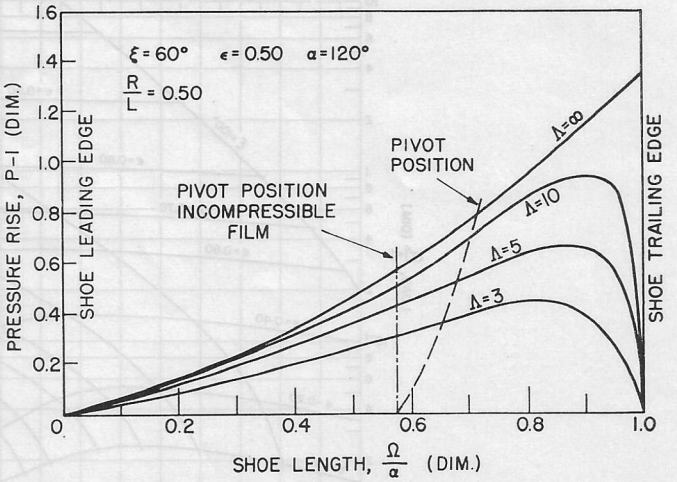

Fig. 2 Circumferential shoe pressure distribution with a fixed film thickness for various values of Λ

In this region, the bearing pressure rise is only slightly above ambient. Thus computer roundoff errors make it difficult to obtain accurate data at low Λ, unless a double precision routine is used, which is time consuming.

Region 2 represents the normal range of gas bearing operation. Fig. 2 illustrates that, as Λ increases, the trailing-edge pressure gradients become very high. Thus, to obtain accurate data in this region, the number of computer grid points must be increased in order to produce a convergent solution. The value of $\Lambda = 20$ represents the practical limit of the computer program because of convergence problems and running time. This difficulty has now been largely overcome by a recent computer program developed by Castelli [4] which utilizes the variable $Q = (PH)^2$. At high Λ-numbers, Q approaches a constant.

The third compressibility region in which $\Lambda > 20$ represents the case where the gas bearing is approaching the asymptotic solution of PH = const. In this region, large changes in Λ result in only small increases in the bearing pressure profile. It will be demonstrated that proper bearing design should avoid this region because of excessive friction losses.

Fig. 2 shows that, for the given film geometry of $\epsilon = 0.5$ and $\xi = 60$ deg, the center of pressure increases from 0.575 when $\Lambda \rightarrow 0$, to 0.71 when $\Lambda \rightarrow \infty$. The influence of compressibility on the shift of the shoe center of pressure is discussed in detail in references [3, 5].

Example:

Let $\epsilon = 0.5$, $\xi = 60$ deg, $R = 1$ in., $\alpha = 120$ deg, $L = 2$ in., $\mu = 2.03 \times 10^{-9}$, $Pa = 6$ psia, $C = 1.0 \times 10^{-3}$ in.

$$\Lambda = \frac{6\mu\omega}{Pa}\left(\frac{R}{C}\right)^2 = 2.63\omega \times 10^{-3} = 2.75 \times 10^{-4} N_{\text{rpm}}$$

The leading-edge film thickness H_L is given by

$$H_L = 1 + \epsilon \cos (\xi) = 1 + 0.5 \cos (60 \text{ deg}) = 1.25$$

$$h_L = CH_L = 1.25 \times 10^{-3} \text{ in.}$$

The trailing-edge film thickness is given by

$$H_T = 1 + \cos (\xi + \alpha) = 1 + 0.5 \cos (180 \text{ deg}) = 0.5$$

$$h_T = CH_T = 0.5 \times 10^{-3} \text{ in.}$$

The bearing load capacity, speed, and center of pressure corre-

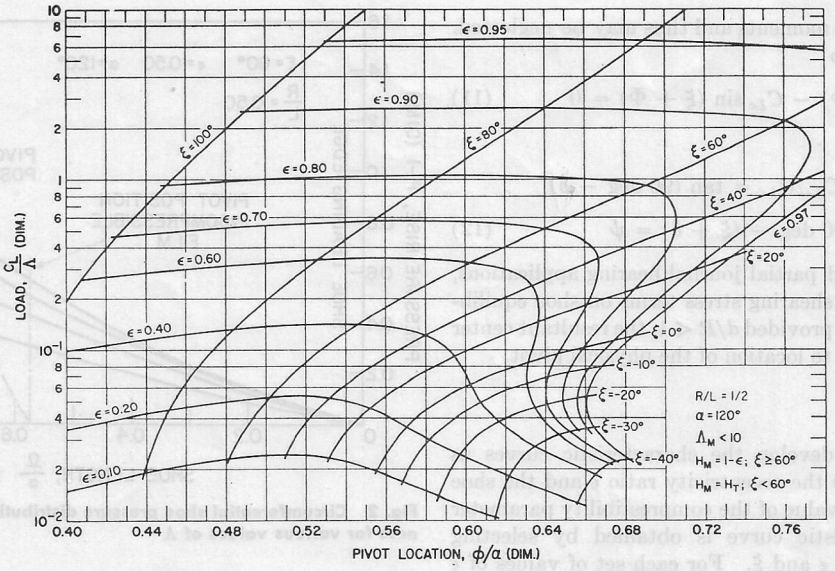

Fig. 3 Load factor versus pivot location. $R/L = 0.50$, $\alpha = 120$ deg, $\Lambda_m < 10$.

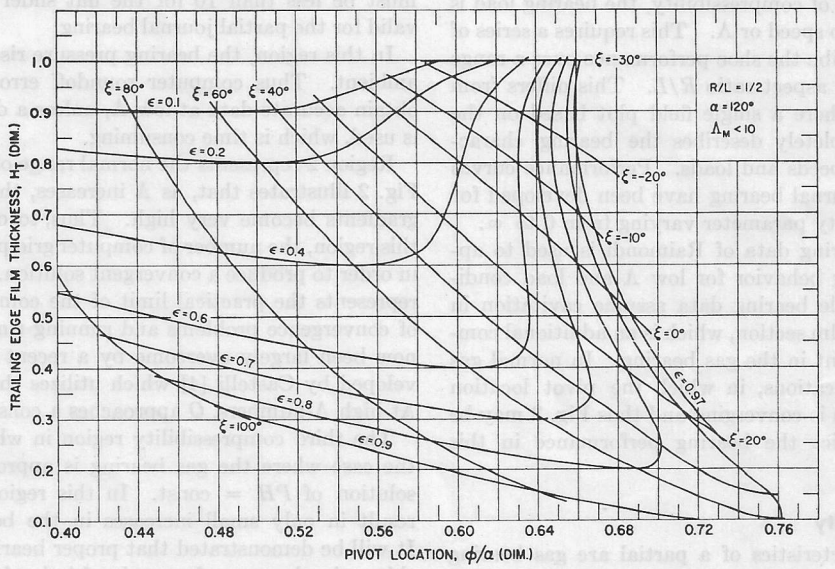

Fig. 4 Trailing-edge film thickness versus pivot location. $R/L = 0.5$, $\alpha = 120$ deg, $\Lambda_m < 10$.

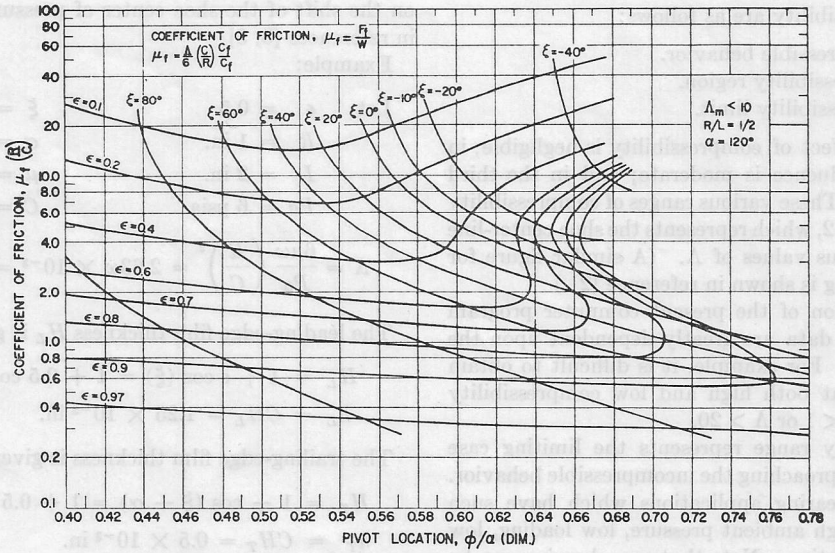

Fig. 5 Coefficient of friction versus pivot location. $R/L = 0.50$, $\alpha = 120$ deg, $\Lambda_m < 10$.

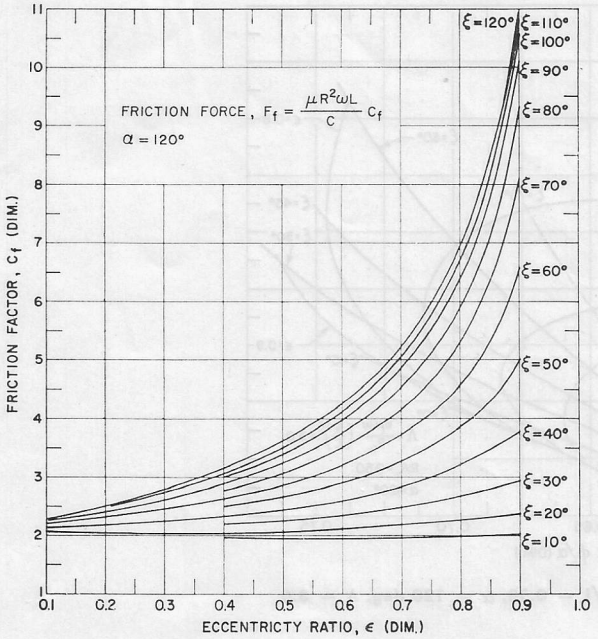

Fig. 6 Approximate friction factor for $\alpha = 120$ deg

sponding to several values of Λ are given in Table 1 (see Figs. 3–10).

In Table 1, we see that, for a fixed film geometry, the center of pressure does not remain constant but increases with speed or compressibility number (see Fig. 2). Also, the maximum load capacity the bearing is capable of supporting in this particular example is slightly over 16 lb. When the rotor speed is increased by a factor of 20, from $\Lambda = 0.5$ to 10, the bearing load capacity is only increased by a factor of 8 due to lubricant compressibility effects.

Bearing Performance at Low Compressibility Numbers

In order to determine the regions in which the compressible and incompressible solutions merge, it is necessary to have bearing field maps for $\Lambda \to 0$.

To represent this region, the data of Raimondi [6] for the 120 deg incompressible bearing were used. Fig. 3 represents the bearing dimensionless load and speed coefficient and is related to the Sommerfeld number used by Raimondi as follows:

$$\frac{C_L}{\Lambda} = \frac{1}{6\pi S} \tag{13}$$

where

$$\text{S} = \text{Sommerfeld number} = \frac{\mu N}{P_j}\left(\frac{R}{C}\right)^2$$

Fig. 4 represents the bearing trailing-edge film thickness corresponding to Fig. 3. With the use of these two figures, the bearing load capacity and minimum film thickness for various shoe pivot positions and values of C_L/Λ may be readily calculated. Examination of Fig. 3 shows that the bearing load capacity is fairly insensitive to pivot location. That is, a pivot position anywhere between $\phi/\alpha = 0.45$ and 0.65 will produce satisfactory results from the standpoint of bearing load capacity. This is in direct contrast to the flat slider bearing, where the load drops off rapidly as the pivot approaches the pad center [7].

Table 2 represents the effect of pivot location on the shoe minimum film thickness for the load factors of $C_L/\Lambda = 0.10$ and 1.0. Table 2 shows that, with an incompressible film, the optimum pivot position to obtain the maximum value of minimum film thickness H_m is approximately between 0.55 and 0.60, depending upon the loading. Raimondi states that a pivot position of 0.60 for the 120 deg bearing will produce optimum results for a wide

Table 1 Bearing load capacity and center of pressure of a fixed partial journal bearing for various values of Λ

Λ	N_{rpm}	Φ/α	C_L	W, lb
0.5	1,820	0.575	0.115	1.38
3.0	11,000	0.65	0.51	6.11
5.0	18,200	0.66	0.66	7.92
10.0	36,400	0.68	0.93	11.15
∞	>100,000	0.71	1.35	16.2

Table 2 Effect of pivot location on the minimum film thickness with an incompressible lubricant

No.	Load	ϕ/α	ϵ	ξ	H_T	H_m
I	$C_L/\Lambda = 1.0$	0.400	0.820	105°	0.420	0.180
	S = 0.0542	0.452	0.802	100°	0.358	0.198
		0.500	0.800	92°	0.330	0.200
		0.660	0.800	66°	0.210	0.200
		0.700	0.815	60°	0.1850	0.1850
		0.765	0.900	41°	0.1490	0.1490
II	$C_L/\Lambda = 0.10$	0.400	0.400	95°	0.68	0.600
	S = 0.542	0.472	0.340	80°	0.68	0.660
		0.528	0.320	60°	0.68	0.680
		0.602	0.43	20°	0.67	0.670
		0.66	0.80	0°	0.60	0.600
		0.70	1.18	−7°	0.54	0.54

Table 3 Comparison between pivot locations for maximum load and minimum coefficient of friction

		60°	120°	180°
ϕ/α	1	0.549	0.554	0.563
	2	0.565	0.571	0.582
Relative Load capacity, %	1	100%	100%	100%
	2	100%	97.4%	97.3%
Relative Friction, %	1	104.5%	103.5%	104.2%
	2	100%	100%	100%

(1) Pivot location for maximum load capacity
(2) Pivot location for minimum coefficient of friction.

range of the Sommerfeld number. It is of interest to note that the optimum pivot position for the flat slider with an aspect ratio of $B/L = 1.0$ [$B/L = (R/L)\,\alpha = 1.048$ for the 120 deg bearing with $R/L = 1/2$] is 0.60.

Another important design consideration is the shoe coefficient of friction as shown in Fig. 5. If the pressure gradient term is neglected in the friction equation, the friction force is a function of film geometry alone as given by Fig. 6. Thus, by use of only ϵ and ξ, it is possible to calculate the shoe friction force with only a 5 to 10 percent error depending upon S. Thus, by use of Figs. 5 and 6 in conjunction with the load capacity curves (Figs. 3, 7–10), the optimum pivot position and clearance ratio for minimum coefficient of friction may be determined.

Optimum Design Conditions at Low Compressibility Numbers

The partial journal bearing may be optimized for either maximum load capacity or minimum coefficient of friction. Table 3, based on data by Kingsbury [8], shows the comparison of the optimum pivot positions for the 60 deg, 120 deg, and the 180 deg infinite-width journal bearings. In general, as the shoe arc length increases, the optimum pivot positions for both maximum load capacity and minimum shoe coefficient of friction increase.

It is important to note that the optimum pivot position for maximum load does not correspond to the optimum value for minimum coefficient of friction. The optimum value for minimum friction is always 5 to 10 percent larger, depending upon the compressibility number. Compressibility effects and side leakage (finite-width bearing) will cause both of these optimum values to increase. Therefore, the values of Table 3 represent the lower bound of the optimum pivot ratios ϕ/α to obtain maximum load or minimum friction losses.

Optimum Design Conditions With Lubricant Compressibility

Fig. 7–10 represent the 120 deg bearing characteristic curves

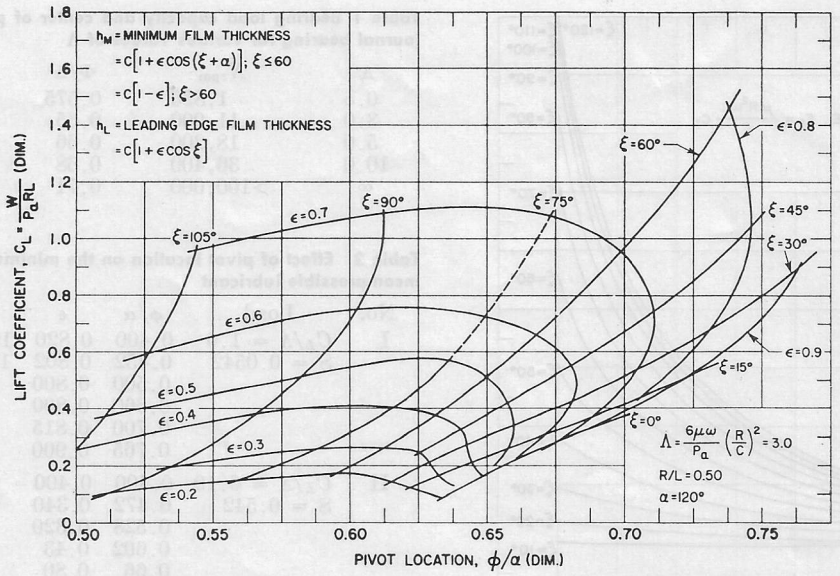

Fig. 7 Load coefficient versus pivot location. $R/L = 0.50$, $\alpha = 120$ deg, $\Lambda = 3.0$.

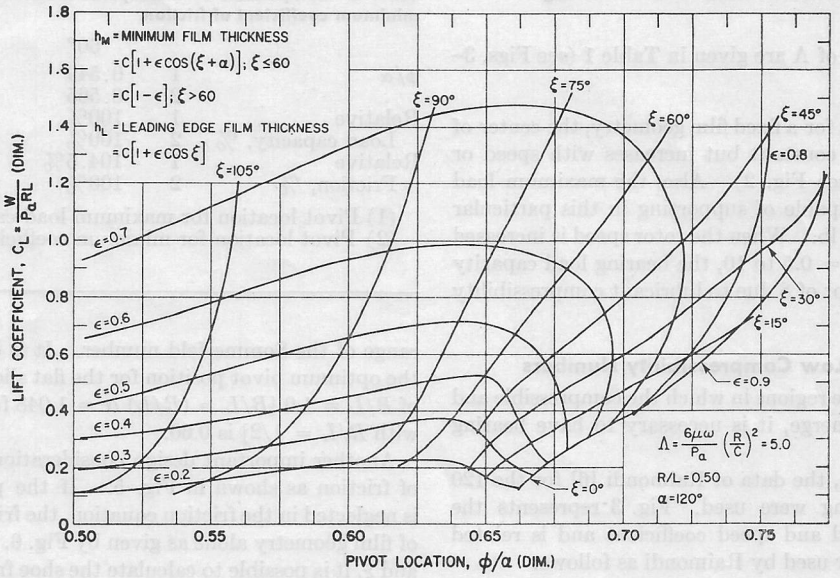

Fig. 8 Load coefficient versus pivot location. $R/L = 0.50$, $\alpha = 120$ deg, $\Lambda = 5.0$.

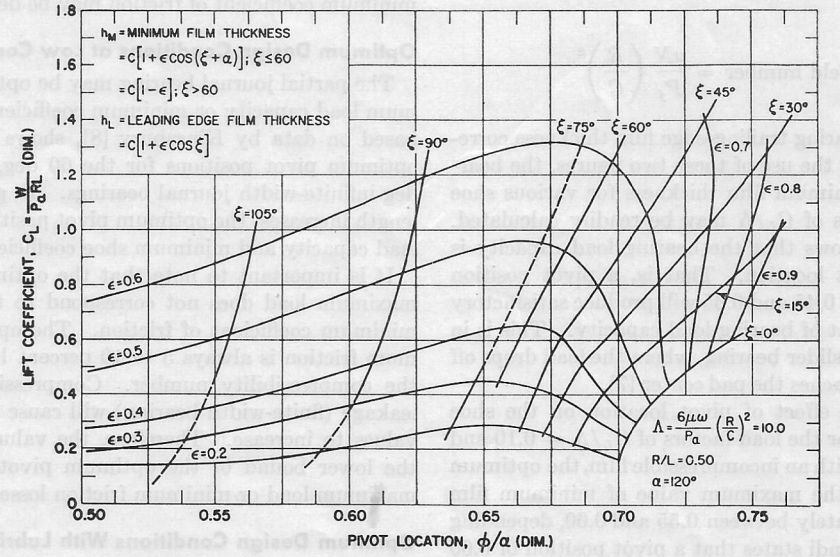

Fig. 9 Load coefficient versus pivot location. $R/L = 0.50$, $\alpha = 120$ deg, $\Lambda = 10.0$.

Table 4 Comparison of various bearing types at optimum loading conditions at low Λ

Bearing type	Pivot position, ϕ/α 60°	120°	Load factor, C_L/Λ_m 60°	120°	Reduction in load, % 60°	120°	Clearance, C/h_m 60°	120°
Optimum clearance bearing	0.55	0.554	0.0319	0.121	0%	0%	3.97	1.93
Fitted Bearing	0.596	0.648	0.0269	0.0721	16%	40%	0	0
Central loaded bearing	0.50	0.50	0.0287	0.107	10%	12%	3.95	1.88

Table 5 Approximate limits of incompressibility for 120 deg bearing

Λ/C_L	C_L	H_m	Λ	Λ_m
1.0	1.2	0.20	1.2	30
4.0	0.8	0.41	3.2	19
9.0	0.4	0.60	3.6	10
12.0	0.2	0.70	2.4	5

for a range of Λ from 3 to ∞. The limiting case of $\Lambda = \infty$ represents the maximum obtainable load capacity that the compressible film is capable of generating. The asymptotic solution for this is given in reference [3]. As the compressibility number increases, the location of the optimum pivot position shifts toward the shoe trailing edge. At high Λ-values, there is a considerable deviation between the load capacity at the optimum pivot position and the central pivot.

By the use of the performance curves, Figs. 3–10, the behavior of a pivoted-pad bearing over the complete range of Λ may be evaluated. Fig. 11 represents the film-thickness characteristics for various load coefficients of a 120 deg bearing pivoted at $\phi/\alpha = 0.65$. It is of interest to note the deviation between the compressible and the incompressible fluid film thickness as Λ increases. If all of the parameters of Λ except angular velocity are held constant, then the constant load lines illustrate how the minimum film thickness increases with increasing speed for a given load.

Fig. 11 shows that an increase in Λ from 5 to 10 for the compressible fluid causes only slight changes in the minimum film thickness. This clearly indicates that, once a certain range of Λ is obtained, little is gained by further increase in the compressibility number. As Λ increases, the compressibility effects increase also, causing a limit to the value of H_m that may be obtained with speed [1]. The maximum attainable value of H_m for a particular value of C_L may be calculated from the $\Lambda = \infty$ field map in Fig. 10.

For the load coefficient of $C_L = 0.4$, the compressible and incompressible solutions merge at approximately Λ 3.0 and $H_m = 0.55$. The value of Λ_m based on minimum film thickness is given by

$$\Lambda_m = \Lambda/H_m{}^2 = 3.0/(0.55)^2 = 9.9$$

Thus, when $\Lambda_m < 10$ for this particular load coefficient, the bearing may be adequately approximated by incompressible lubrication theory.

The data represented in Fig. 11 may be expressed in an alternate form in which the abscissa is the parameter Λ/C_L or the familiar Sommerfeld number which is so frequently used in the analysis of oil-lubricated bearings. The use of the Sommerfeld number enables one to express the incompressible load capacity of a tilting-pad journal bearing by a single curve as shown in Fig. 12. Examination of Fig. 12 shows the regions in which the compressible and incompressible solutions merge, and these values are tabulated in Table 5 for various load coefficients.

To determine the influence of clearance only on the bearing performance, we proceed as follows. Using the value of $\Lambda/C_L = 30$ as a starting reference, we assume the reference clearance to be C_0. To obtain the clearance value at any other performance number, we have

$$C = C_0 \left(\frac{30}{\Lambda/C_L}\right)^{1/2} = 5.49 \sqrt{\frac{C_L}{\Lambda}}\, C_0 \qquad (14)$$

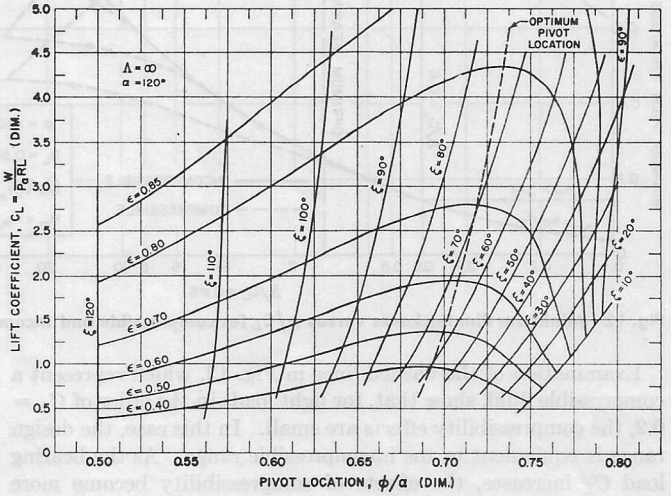

Fig. 10 Load coefficient versus pivot location. $\alpha = 120$ deg, $\Lambda = \infty$

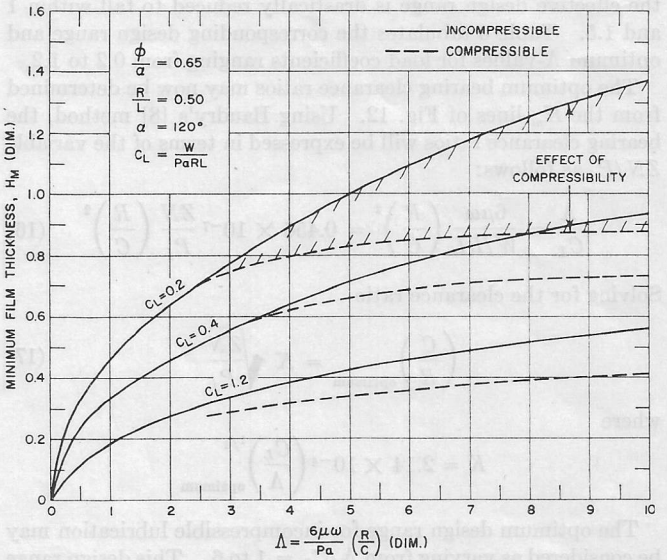

Fig. 11 Minimum film thickness versus Λ for compressible and incompressible cases

The corresponding minimum film thickness is given by

$$Hm = \left(\frac{hm}{Co}\right) = \frac{C}{Co}\left(\frac{hm}{C}\right) = 5.49\, Hm \sqrt{\frac{C_L}{\Lambda}} \qquad (15)$$

Evaluation of the maximum value of the H_m-lines will determine the optimum design value of the Sommerfeld number. For example, the solid line which represents the incompressible lubricant indicates that the optimum value of Λ/C_L is 1.5. Examination of the entire curve reveals that satisfactory performance can be obtained over a considerable range of Λ/C_L from 1.0 to 10. This implies that the permissible variation in bearing machined in clearance C is a factor greater than 3 for an incompressible lubricant.

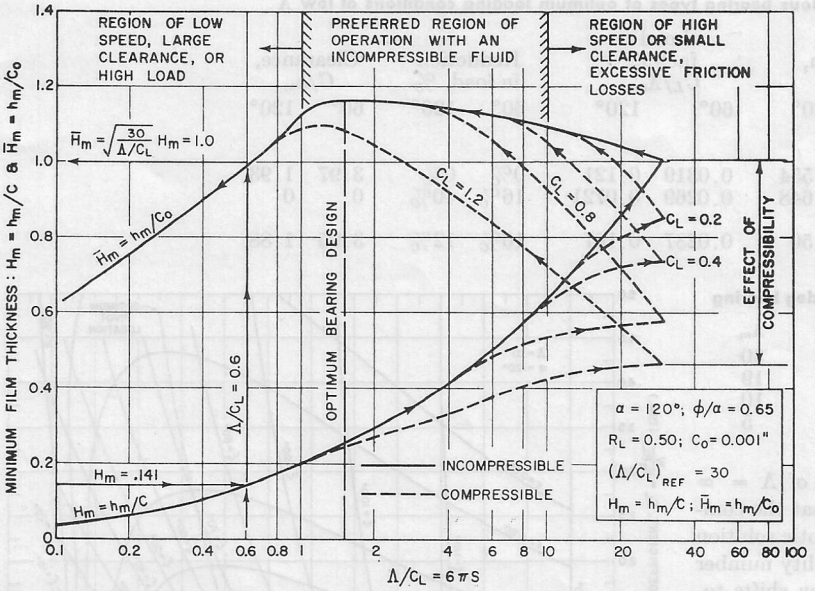

Fig. 12 Minimum film thickness versus Λ/C_L for compressible and incompressible cases

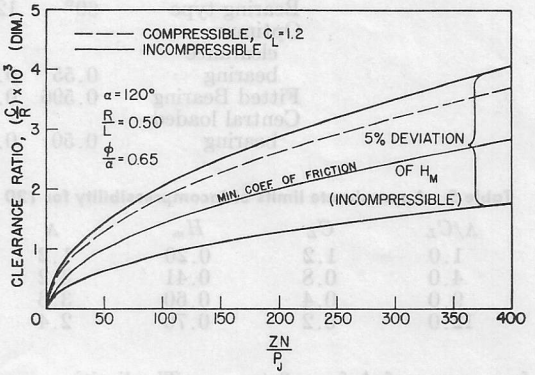

Fig. 13 Optimum clearance ratio for maximum load capacity and minimum coefficient of friction

Examination of the dashed lines in Fig. 12, which represent a compressible fluid, show that, for light loads in the order of $C_L = 0.2$, the compressibility effects are small. In this case, the design range is equivalent to the incompressible range. As the bearing load C_L increases, the effects of compressibility become more pronounced, limiting the preferred bearing design range. For example, Fig. 12 shows that the design range (Λ/C_L) for $C_L = 0.2$ is between 1 and 10, but, if the load is increased to $C_L = 1.2$, the effective design range is drastically reduced to fall within 1 and 1.5. Table 6 tabulates the corresponding design range and optimum Λ-values for load coefficients ranging from 0.2 to 1.2.

The optimum bearing clearance ratios may now be determined from the H_m-lines of Fig. 12. Using Baudry's [8] method, the bearing clearance ratios will be expressed in terms of the variable ZN/P_j as follows:

$$\frac{\Lambda}{C_L} = \frac{6\mu\omega}{W/RL}\left(\frac{R}{C}\right)^2 = 0.456 \times 10^{-7}\frac{ZN}{P_j}\left(\frac{R}{C}\right)^2 \tag{16}$$

Solving for the clearance ratio

$$\left(\frac{C}{R}\right)_{\text{optimum}} = K\sqrt{\frac{ZN}{P_j}} \tag{17}$$

where

$$K = 2.14 \times 10^{-4}\left(\frac{C_L}{\Lambda}\right)^{1/2}_{\text{optimum}}$$

The optimum design range for incompressible lubrication may be considered as varying from $\Lambda/C_L = 1$ to 6. This design range causes only a 5 percent variation in the minimum film thickness. The optimum design value for the compressible bearing with a load coefficient of $C_L = 1.2$ is 1.4. Note that any variation from this design value causes a rapid reduction in the minimum film thickness.

The design clearance ratio range for incompressible lubrication is given by

$$\left(\frac{C}{R}\right)_{\Lambda\to 0} = [0.875 - 2.14] \times 10^{-4}\sqrt{\frac{ZN}{P_j}} \tag{18}$$

and the optimum clearance ratio for the gas bearing for $C_L = 1.2$ is given by

$$\left(\frac{C}{R}\right)_{C_L=1.2} = 1.85 \times 10^{-4}\sqrt{\frac{ZN}{P_j}} \tag{19}$$

By similar calculations, the clearance ratio for minimum coefficient of friction at low Λ is determined to be

$$\left(\frac{C}{R}\right)_{\min C_f} = 1.4\sqrt{\frac{ZN}{P_j}} \tag{20}$$

The plots of the optimum clearance ratio for maximum load capacity and minimum coefficient of friction are shown in Fig. 13. Note that, for low Λ or incompressible behavior, the permissible variation of the design clearance may be a factor of 2.5. In the case of the gas bearing, the permissible clearance variation reduces sharply with increased loading.

Sample Calculation

As an illustration of equation (19) to calculate the bearing optimum clearance ratio for maximum H_m, this example is given:

Assume

$C_L = 1.2$ $\quad N = 60{,}000$ rpm
$R = 1$ in. $\quad \mu = 2.63 \times 10^{-9}$ lb-sec/sq in.
$L = 2$ in. $\quad \alpha = 120°$
$P_a = 6$ psia $\quad \phi/\alpha = 0.65$

$$W = C_L P_a RL = (1.2)(6)(1)(2) = 14.4 \text{ lb}$$

$$P_j = \frac{W}{DL} = \frac{14.4}{(2)(2)} = 3.6$$

$$\frac{ZN}{P_j} = \frac{(2.61 \times 10^{-9})\ (60{,}000 \text{ rpm})}{(1.45 \times 10^{9}) \times 3.6} = 300$$

$$\frac{C}{R} = 1.85 \times 10^{-4}\sqrt{\frac{ZN}{P_j}} = 3.2 \times 10^{-3} \text{ in/in.}$$

The permissible variation in clearance ratio for the oil film bearing with the same (ZN/P_j)-value is 1.5 to 3.7 mils/in.

Conclusions

The performance of a gas-lubricated partial journal bearing may be estimated by incompressible theory for certain ranges of the Sommerfeld number.

Table 6 Preferred design conditions for 120 deg bearing

Load C_L	Design range, Λ/C_L	Design range, Λ	Optimum value, Λ
0.2	1–10	0.2–2.0	0.4
0.4	1–7	0.4–2.8	0.8
0.8	1–4	0.8–3.0	1.5
1.2	1–1.5	1.2–1.8	1.5

At low compressibility numbers, a considerable variation in shoe pivot position and Sommerfeld number is permissible. The bearing load capacity is relatively insensitive to pivot location.

The bearing pivot position may be optimized for either minimum coefficient of friction or maximum film thickness H_m for a given load. The location of the optimum pivot for minimum coefficient of friction is always 5 to 10 percent greater than the optimum value for maximum film thickness.

As the compressibility number increases, the optimum pivot locations increase toward the shoe trailing edge. Shoe side leakage or reduction of aspect ratio also causes, in general, an increase in the optimum pivot positions.

At high compressibility numbers, the tilting-pad load capacity and shoe friction vary greatly with the pivot position.

For an incompressible lubricant, the bearing clearance ratio may vary by a factor of 3 and still maintain satisfactory bearing load capacity. In the case of a gas bearing, the permissible variation in clearance decreases rapidly with loading. The optimum design value of Λ for a wide range of loads is approximately 1.5. Values of $\Lambda > 5$ should be avoided because of excessive friction losses.

Acknowledgment

The work reported herein was conducted under the sponsorship of the U. S. Atomic Energy Commission, under Contract AT(30-1)-2512, task 3 at The Franklin Institute. The author also wishes to acknowledge the support of the Research Laboratories for Engineering Science of the University of Virginia for its assistance in the development of this work.

References

1 W. A. Gross, *Gas Film Lubrication*, John Wiley & Sons, Inc., New York, N. Y., 1962.

2 V. Castelli, C. H. Stevenson, and E. J. Gunter, Jr., "Steady-State Characteristics of Gas-Lubricated, Self-Acting, Partial-Arc Journal Bearings of Finite Width," *ASLE Trans.*, vol. 7, 1964, pp. 153–167.

3 E. J. Gunter, Jr., J. G. Hinkle, and D. D. Fuller, "The Effects of Speed, Load, and Film Thickness on the Performance of Gas-Lubricated Tilting-Pad Journal Bearings," *ASLE Trans.*, vol. 7, no. 4, 1964, pp. 353–365.

4 V. Castelli and J. Pirvics, "Equilibrium Characteristics of Axial-Groove Gas Lubricated Bearings," presented ASLE-ASME Lub. Conf., San Francisco, October 18, 1965.

5 E. J. Gunter, Jr., J. G. Hinkle, and D. D. Fuller, "Design Guide for Gas-Lubricated Tilting-Pad Journal and Thrust Bearings With Special Reference to High-Speed Rotors," NYO-2512-1, The Franklin Institute, I-A2392-3-1, November, 1964.

6 A. A. Raimondi, "A Theoretical Study of the Effect of Offset Loads on the Performance of a 120° Partial Journal Bearing," *ASLE Trans.*, vol. 2, no. 1, pp. 147–157.

7 A. A. Raimondi and J. Boyd, "Applying Bearing Theory to the Analysis and Design of Pad-Type Bearings," TRANS. ASME, vol. 77, 1955, pp. 287–309.

8 A. Kingsbury, "Optimum Conditions in Journal Bearings," TRANS. ASME, vol. 1932, pp. 123–148.

9 R. Baudry and T. M. Tichvinsky, "Journal Bearing Performance," *Journal of Applied Mechanics*, vol. 2, TRANS. ASME, vol. 57, 1935, pp. A-121–A-127.

DISCUSSION

G. Pitts[2]

It is encouraging to see yet another paper by the author added to the careful study he has already made of the pivoted-pad bearing. The conclusions he draws on the relationship between load capacity and bearing friction are both useful and interesting, as are those on fluid compressibility.

As he points out, the limitations on the direct numerical method of solution are: computation time, stable convergence at high Λ, and the number of design charts required to cover the complete design range. The present report goes a long way to overcome the need for design charts at high Λ, but is unable to satisfy the latter limitation.

I would like to draw attention to an analytical method of solution, outlined in the paper by the discusser,[3] and improved in a later paper.[4] The solution by this method is obtained for a bearing pad of infinite length, and corrected for a finite pad by means of an end flow factor. It enables design curves to be plotted in terms of pivot position, and a dimensionless load, which is independent of L/R. There is no stability limit on high compressibility numbers, and the computation time required for each set of design curves is very short. The curves were programmed in Algol, on an I.C.T. 1909 computer, and each set of curves took less than five minutes to produce, and often less than one minute. This solution is very accurate at high compressibility numbers, and quite accurate in the region covered by the curves obtained by Dr. Gunter.

In Dr. Gunter's section on load capacity reference is made to the radial position of the pivot. I think, in fact, the point about which frictional shearing forces are zero would be at some position away from the journal surface. It would, however, seem preferable to keep the pivot as near the journal surface as possible, in order that any shearing moments would tend to make the pad pitch trailing edge down, and thus reduce the possibility of "lock-up."

The author appears to have experienced some difficulty in computing pressure distributions at low compressibility numbers due to computer round-off errors. The technique employed in the two papers[3,4] was to perform the computation in terms of dimensionless gauge pressures. This means that for small pressures the values are stored accurately in floating point form by the computer. If β were set equal to 1 in equation (5), this equation would then be in a gauge pressure form. I should be interested to know if the author has already pursued this point.

I think the author would agree that the curves of friction coefficient should be used as a guide rather than as absolute values. The author,[5] together with his colleagues, has compared experimental and theoretical values of friction, giving power losses of 0.87 hp and 0.219 hp, respectively. On the test rig in question, windage losses were included in the experimental value, and could not be separated. At Southampton I have a rig on which friction losses can be measured independently of windage [4], and I have found that actual losses are about double the predicted losses, which would suggest that only about half the experimental losses quoted in the paper by the authors[5] are due to windage.

A final point I would like to make is on optimum bearing design. The paper mentions design for minimum friction conditions, and maximum load, but an important criterion in bearing design is bearing stiffness. I realize the difficulties involved in computing the pivot film stiffness of a tilting pad bearing, but I have found experimentally that the pivot position for maximum stiffness does not concide with that for maximum load. I would be interested to know the author's views on the subject.

[2] Research Fellow, Department of Mechanical Engineering, University of Southampton, England.

[3] G. Pitts, "An Analytical Study of the Tilting-Pad Gas Lubricated Journal Bearing," *I. Mech. E. Proceedings*, vol. 181, part 1, paper 13, 1966–1967.

[4] G. Pitts, "Design Charts for Partial Arc Gas Journal Bearings," Gas Bearing Symposium, Southampton University, April, 1967.

[5] E. J. Gunter, Jr., J. G. Hinkle, and D. D. Fuller, "The Effects of Speed, Load and Film Thickness on the Performance of Gas-Lubricated, Tilting-Pad Journal Bearings," *A.S.L.E. Transactions*, vol. 7, 1964, pp. 353–365.

Authors' Closure

Mr. Pitts has presented several important factors concerning the difficulty of obtaining extensive bearing data to be used by the engineer for design purposes. Because of the computer time required to produce the bearing performance curves, only

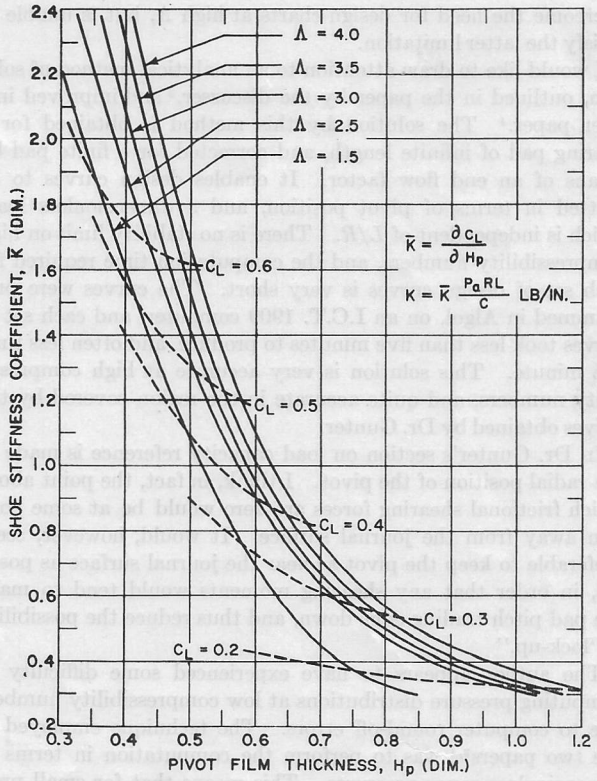

Fig 14

several ranges of bearing aspect ratio were investigated. Therefore, because of the large number of variables involved, it would be invaluable to the designer to have closed form approximate expressions to predict the bearing behavior for various values of pivot location, aspect ratio, and speed.

The analysis presented by Mr. Pitts in predicting the approximate bearing load capacity should be of considerable value to the designer in preliminary bearing selection. Mr. Pitts, in his analysis has used Ausman's linearized PH equation which will introduce some approximation in his results. The deviation to be expected with the linearized Reynold's equation will be dependent on the compressibility parameter, Λ.

As Mr. Pitts has indicated, some difficulty was encountered in computing pressure distributions for low compressibility numbers. This difficulty was somewhat avoided by using a double precision computer routine, but has now been corrected by reprogramming equations in terms of dimensionless gage pressure. In our experimental work, we were not able to obtain accurate friction characteristics as it was masked by the windage losses of the rotor. The experimental measurements of the bearing load capacity agreed within 10 percent of the predicted values, and I would expect the bearing losses to be of the same order of accuracy.

The bearing pivot film stiffness is an important factor in the evaluation of the dynamical characteristics of a complete tilting pad bearing. The pad stiffness was obtained for the 120 deg bearing for various pivot locations and it was noted that pivot position has considerable influence on pad stiffness for constant values of r and hp. Fig. 14 represents the dimensionless shoe stiffness vs pivot film thickness for the 120 deg bearing with the pivot position at $\phi/\alpha = {}^2/_3$. Note that Fig. 14 shows that the pivot film stiffness is greatly influenced by bearing load as well as speed. Our limited evaluation of optimum pivot location for maximum stiffness indicates that the pivot position should be slightly greater than the optimum pivot position for maximum load capacity, and that this value increases slightly as the compressibility parameter Λ increases, or as the shoe aspect ratio R/L reduces.